Journal of Photochemistry & Photobiology, B: Biology 164 (2016) 323–334

Contents lists available at ScienceDirect

Journal of Photochemistry & Photobiology, B: Biology

journal homepage: www.elsevier.com/locate/jphotobiol

Comparative study on the interaction of two binuclear Pt (II) complexes with human serum albumin: Spectroscopic and docking simulation assessments

Mohammad Bagher Shahsavani [a,b], Shamseddin Ahmadi [b], Marzieh Dadkhah Aseman [c], S. Masoud Nabavizadeh [c], Mohammad Mehdi Alavianmehr [d], Reza Yousefi [a,*]

[a] Protein Chemistry Laboratory (PCL), Department of Biology, College of Sciences, Shiraz University, Shiraz, Iran
[b] Department of Biological Science and Biotechnology, Faculty of Science, University of Kurdistan, Sanandaj, Iran
[c] Department of Chemistry, College of Sciences, Shiraz University, Shiraz, Iran
[d] Department of Chemistry, Shiraz University of Technology, Shiraz, Iran

ARTICLE INFO

Article history:
Received 12 August 2016
Received in revised form 26 September 2016
Accepted 27 September 2016
Available online 30 September 2016

Keywords:
Binuclear Pt (II) complexes
Human serum albumin
Fluorescence study
Circular dichroism

ABSTRACT

Human serum albumin (HSA) principally tasks as a transport carrier for a vast variety of natural compounds and pharmaceutical drugs. In the present study, two structurally related binuclear Pt (II) complexes containing *cis*, *cis*-[Me_2Pt (μ-NN) (μ-dppm) $PtMe_2$] (**1**), and *cis*, *cis*-[Me_2Pt(μ-NN)(μ dppm) Pt($(CH_2)_4$)] (**2**) in which NN = phthalazine and dppm = bis (diphenylphosphino) methane were used to investigate their interaction with HSA, using UV–Vis absorption spectroscopy, fluorescence, circular dichroism and molecular dynamic analyses. The spectroscopic results suggest that upon binding to HSA, the binuclear Pt (II) complexes could effectively induce structural alteration of this protein. These complexes can bind to HSA with the binding affinities of the following order: complex **2** > complex **1**. Moreover, the thermodynamic parameters of binding between these complexes and HSA suggested the existence of entropy-driven spontaneous interaction, which mostly dominated with the hydrophobic forces. The ANS fluorescence results also indicated that two binuclear Pt (II) complexes were competing for the binding to the hydrophobic regions on HSA. In addition, competitive displacement assay and docking simulation study revealed that complexes **1** and **2** bind to the drug binding sites II and I on HSA, respectively. Furthermore, complex **2**, with the higher binding affinity for HSA, shows more denaturing effect on this protein. Considering the protein structural damages in the pathway of harmful side effects of platinum drugs, complex **1** with the moderate binding affinity and low denaturing effect might be of high significance.

1. Introduction

During the past decades, platinum complexes have been successfully applied in the clinical practice for the treatment of several solid tumors [1]. These organometallic complexes are believed to induce apoptosis in cancer cells through the damaging interaction with DNA as their final target molecule [2]. However, prior to exerting their damaging effects on DNA, they may also interact with a number of proteins and peptides either in the blood stream or in intracellular milieu [3]. The interaction between drugs and plasma proteins is an essential pharmacological parameter, which may strongly influence their pharmacodynamics. This interaction may have an important effect on the delivery and removal of drugs, as well as on structure and physiological action of the carrier proteins [4,5]. However, the complications associated with adsorption, distribution, metabolism, and elimination (ADME) are motivating the scientists to look for the new strategies with the aim to enhance these features at the initial phase of drug design.

One of the most significant factors capable of altering ADME of new drugs is their administered concentration and their binding affinity toward human serum albumin (HSA). On the other hand, the drugs with lower effective concentration (lower IC_{50}) and moderate binding affinities are potentially important to conquer the problems associated with ADME. HSA is the most abundant carrier protein in human blood stream which widely used in many studies because of its well-known primary and tertiary structures [6]. HSA plays a significant role in the transportation of many endogenous and exogenous substances, drugs, and other biologically active compounds present in the bloodstream [7]. As indicated in Fig. 1A, this heart-shaped protein composed of three structurally similar domains I-III. Each domain of this protein consists of two subdomains (A & B) stabilized by 17 disulfide bridges [8–11]. Crystal structure analyses suggest that HSA has binding sites for both aromatic and heterocyclic ligands within two well-known pockets in subdomains IIA and IIIA; generally referred to them drug binding sites I and II, respectively. Both

* Corresponding author.
E-mail address: ryousefi@shirazu.ac.ir (R. Yousefi).

http://dx.doi.org/10.1016/j.jphotobiol.2016.09.035
1011-1344/

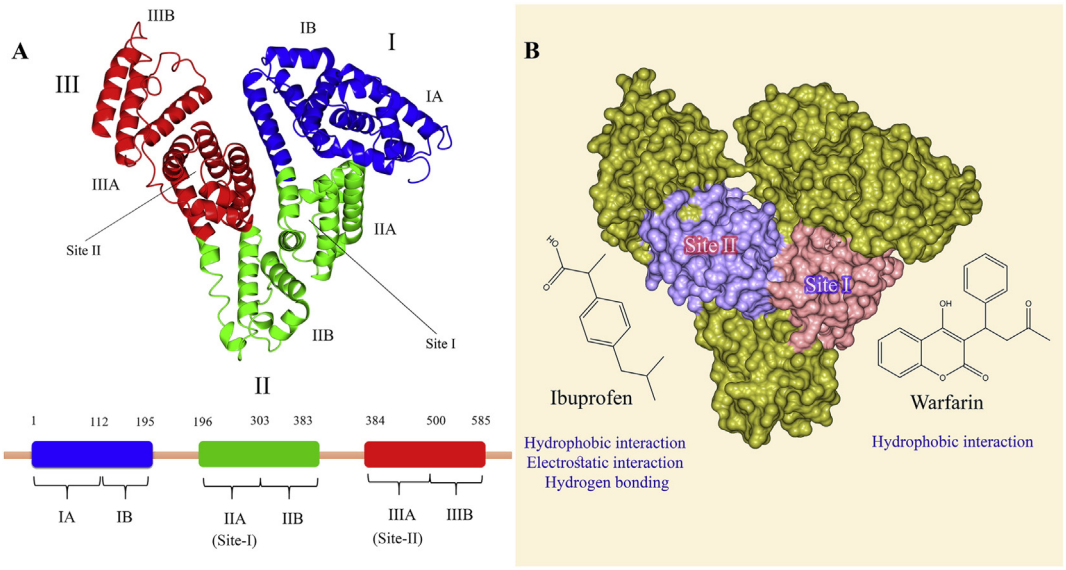

Fig. 1. A) Schematic illustration of domain structural organization and position of two drug binding sites I and II on HSA. B) HSA and two drug site markers frequently used for the competitive binding analyses of ligands to sites I and II.

hydrophobic and electrostatic interactions play a major role in controlling the affinity toward these protein-binding sites [10,11]. While several hydrophobic residues participate in shaping the drug binding site I; the residues with hydrophobic, polar and charged characteristics are participating in shaping drug binding site II [8,10–12].

Consequently, it is suggested that drugs with dominant hydrophobic characters may possess higher affinity toward drug binding site I and those capable of forming strong electrostatic interaction and hydrogen bonding may interact with site II. For instance, as shown in Fig. 1B two known classical drugs warfarin and ibuprofen, preferentially bind to the sites I and II, respectively. Warfarin has more hydrophobic character while ibuprofen can also participate in hydrogen bonding and electrostatic interaction. According to the previous reports, binding of various drugs to HSA can alter the ADME [13]. Consequently, this interaction is significant to control drug delivery, drug storage and limitation of drug's rapid metabolism [14]. In addition, when hydrophobic drugs bind to HSA, their apparent solubility may be improved [15,16]. Previous studies revealed that when Pt compounds are robustly bound to plasma proteins e.g., HSA, they get efficiently deactivated and eliminated from the body, therefore never reach DNA as their ultimate site of action.

Moreover, the interaction with drugs/Pt complexes which results in conformational changes/unfolding of HSA, may disturb the protein's biological functions and can elucidate the thinkable therapeutic side effects related to administration of some drugs [3,13,16]. For this purpose, studying the interaction of Pt complexes, which can improve ADME, with HSA is of the great essentiality. In the current study, HSA was used to evaluate the interaction between this protein and two structurally related binuclear Pt (II) complexes, which contain: *cis*, *cis*-[Me_2Pt (μ-NN) (μ-dppm) $PtMe_2$] (**1**), and *cis*, *cis*-[Me_2Pt(μ-NN)(μ dppm) $Pt(CH_2)_4$)] (**2**) in which NN = phthalazine and dppm = bis (diphenylphosphino) methane (Fig. 2A). According to results of our previous study, these complexes indicate a significant anticancer activity against cancer cell lines [17]. In this study, the binding of binuclear Pt (II) complexes to HSA, thermodynamics parameters of the interactions and the protein structural changes induced by the synthetic complexes were assessed using different spectroscopic methods. Moreover, molecular docking simulation (MDS) was performed to define their binding affinity and binding sites on human serum albumin.

2. Material and Methods

2.1. Materials

Human serum albumin (HSA) was purchased from Sigma. All other materials and reagents obtained from Sigma-Aldrich Co, and were of the analytical grade. The concentration of HSA was determined spectrophotometrically using a molar absorptivity of 36,000 M^{-1} cm^{-1} at 280 nm. All solutions were prepared in double-distilled water. In addition, most of the binding assessments were carried out in 5 mM Tris-HCl buffer pH 7.4, containing 50 mM NaCl (TN buffer).

2.2. Methods

2.2.1. Synthesis of the Binuclear Pt (II) Complexes

The binuclear Pt (II) complexes were synthesized as described previously [18,19]. In brief, to a solution of *cis*, *cis*-[$Me_2Pt(\mu\text{-}SMe_2)(\mu\text{-}dppm)PtR_2$] (R = Me or $(CH_2)_4$) in acetone (15 mL) was added phthalazine, at room temperature. The mixture was stirred for 1 h, the solvent was then removed under reduced pressure, and the residue was triturated with ether (3 mL) to give final product *cis*, *cis*-[$Me_2Pt(\mu\text{-}NN)(\mu\text{-}dppm)PtMe_2$], complex **1**, and *cis*, *cis*-[$Me_2Pt(\mu\text{-}NN)(\mu$ dppm) $Pt((CH_2)_4)$], complex **2**, which were separated and dried under vacuum. These complexes were fully characterized and confirmed by multinuclear (^1H, ^{31}P, ^{195}Pt) NMR spectroscopy (Fig. 2A) [18,19]. In addition, the synthesized complexes were examined for their anticancer activities using 3-(4,5-dimethylthiazol-2-yl)-2,5-diphenyltetrazolium bromide (MTT) assay [13].

2.2.2. UV–Vis Spectroscopy Analysis

The UV–Vis measurements of HSA were recorded in the range of 200–400 nm at 298 K after incubation of the protein sample with these complexes for 5 min, using a CE 7200 UV–Vis spectrophotometer instrument (Cecil Instruments Ltd., UK). The HSA concentration was fixed at 10 μM and concentration of drug varied between 0 and 18 μM [13]. The experiments were done in TN buffer.

2.2.3. Intrinsic Fluorescence Measurements

The fluorescence measurements were carried out on a Carry-Eclipse spectrofluorimeter (Model Varion, Australia) equipped with an

automatic temperature controller. The excitation wavelength was set at 295 nm to avoid the contribution from tyrosine residues. The emission spectra were collected between 300 and 500 nm. Also, the slit widths were fixed at 5 and 10 nm for excitation and emission, respectively. To perform fluorescence titration experiment, a fixed concentration of HSA (3 μM) was treated with increasing amounts of each binuclear Pt (II) complex in the range of 0–21 μM. Additionally, synchronous fluorescence spectra of HSA (3 μM) with various concentrations of binuclear Pt (II) complexes (0–18 μM) were obtained ($\Delta\lambda = 15$ nm and $\Delta\lambda = 60$ nm) with the excitation and emission slit widths of 5 and 10 nm, respectively.

2.2.4. Determination of Quenching Mechanism

In order to elucidate the mechanism of HSA fluorescence quenching by binuclear Pt (II) complexes, the fluorescence experiments were carried out at 288, 303, and 310 K, where HSA does not undergo important thermal denaturation. The decrease in fluorescence intensity at λ_{max} was analyzed using Stern–Volmer equation [20]:

$$F_0/F = 1 + K_q\tau_0[Q] = 1 + K_{sv}[Q] \quad (1)$$

where F_0 and F are the fluorescence intensities without and with a quencher (binuclear Pt(II) complexes), respectively. Also, K_q and τ_0 correspondingly stand for the rate constant of quenching process and biomolecule average lifetime without a quencher ($\tau_0 = 10^{-8}$ s). Moreover, the K_{sv} is the Stern–Volmer quenching constant, and [Q] is the concentration of the binuclear Pt(II) complexes.

2.2.5. Calculation of Association Constant and Number of Binding Sites

The association constant (K_b) and number of binding sites (n) for binding of small molecules to set of equivalent sites on a macromolecule can be determined using the modified Stern–Volmer equation:

$$\log F_0 - F/F = \log K_b + n\log[Q] \quad (2)$$

where F_0 and F are the fluorescence intensities of HSA in the absence and presence of the quencher (binuclear Pt(II) complexes), respectively, K_b is the association constant, and n indicates the number of binding sites per HSA [25]. The values of n and K_b were obtained from the slope and intercept of the modified Stern–Volmer plot, respectively.

2.2.6. Thermodynamic Study of the Binding Process

In order to clarify the nature of the interaction between binuclear Pt (II) complexes and HSA, the association constant of binuclear Pt (II) complexes was determined at different temperatures (288, 303 and 310 K). The thermodynamic parameters of binding, entropy change ($\Delta S°$) and enthalpy change ($\Delta H°$), were obtained from van't Hoff equation [4]:

$$\ln K_b = -\Delta H^\circ/RT + \Delta S^\circ/R \quad (3)$$

where K_b is the association constant at the given temperature and R is the universal gas constant. The values of $\Delta S°$ and $\Delta H°$ can be obtained from the intercept and slope of the van't Hoff plot, respectively. The free energy changes of the interaction ($\Delta G°$) can be calculated according to the following equation [3]:

$$\Delta G^\circ = -RT\ln K_b \quad (4)$$

2.2.7. Protein Surface Hydrophobicity Analysis

In order to elucidate the role of hydrophobicity on HSA/Pt (II) complex interactions, ANS binding analysis was studied in the absence and presence of these binuclear Pt (II) complexes. The fixed concentrations of HSA (3 μM) and ANS (200 μM) were incubated for 20 min at 25 °C in dark condition. The binuclear Pt (II) complexes were added to the mix solutions of HSA–ANS and after 5 min the excitation of ANS at 365 nm was performed. The band slits for excitation and emission were 5 and 10 nm, respectively [3].

2.2.8. The Competitive Binding Assay

In order to clarify the binding sites of binuclear Pt (II) complexes on HSA, the competitive binding analysis performed in the presence of two already known drugs, warfarin and ibuprofen. Warfarin and ibuprofen are two site markers; respectively specific for drug binding sites I and II on HSA [21]. The concentrations of HSA and warfarin/ibuprofen were kept at 3 μM while binuclear Pt (II) complexes (0–15 μM) were gradually added to the solution of HSA-warfarin/ibuprofen. The fluorescence intensity recorded in the range of 300–500 nm and the excitation wavelength was selected at 295 nm. The association constant was assessed by the modified Stern–Volmer equation [7]:

$$\frac{F_0}{F_0 - F} = \frac{1}{f_a K_a}\,\frac{1}{[Q]} + \frac{1}{f_a} \quad (5)$$

where K_a is the modified Stern–Volmer association constant for the accessible fluorophores, f_a stands for the fraction of accessible fluorescence, F_0 indicates the fluorescence intensity of HSA without binuclear Pt (II) complex, F is the fluorescence intensity of HSA solution containing binuclear Pt (II) complex and site marker and [Q] shows the concentration of binuclear Pt(II) complexes. The values of K_a and f_a were obtained respectively from the slope and intercept of $F_0/(F_0 - F)$ versus 1 / [Q] [13].

2.2.9. Circular Dichroism (CD) Spectroscopy Experiments

The CD spectra after interaction of each binuclear Pt (II) complex with HSA were recorded on a JASCO (J-810) CD spectropolarimeter. Far-UV region (195–260 nm) was selected to investigate the HSA secondary structures and Near-UV region (260–350) was selected to analyze the tertiary structure of this protein using 1 mm path cuvette. The concentrations of HSA in Far and Near-UV CD assessments were 0.2 and 1 mg/mL, respectively. The experiments were done with different concentrations of each binuclear Pt (II) complex as 0, 5, 10, 20, 40 μM. All CD spectra were corrected with their corresponding blank solutions, with the same concentration of binuclear Pt (II) complexes in TN buffer, lacking HSA. All measurements were carried out at 298 K with thermostatically controlled cell holder. Each spectrum was the accumulation of five successive measurements and the data were expressed as molar residue ellipticity [θ] (deg.cm^2.dmol^{-1}) which is defined as the following equation [22]:

$$[\theta] = \frac{MRW \times \theta_{obs}}{10 \times d \times C} \quad (6)$$

where MRW is the mean amino acid residue weight of the HSA, θ_{obs} is the observed ellipticity in degrees at a given wavelength, d stands for the length of the cuvette in cm and C represents the concentration of the protein in mg/mL. The secondary structure alteration of HSA was predicted by CDNN Secondary Structure Analysis software [23].

2.2.10. Molecular Dynamic Simulation

Molecular dynamic simulation of HSA with PDB entry code 4L8U was performed by GROMACS 4.6.5 package [26–28]. The initial structure consists chain A which was complexed with 9-aminocamptothecin. The ligand was removed from the workspace with CCP4 molecular-graphics program version 2, then the HSA topology and interaction parameters were generated, using GROMOS96 43a1 force field [29]. After that the protein was placed in a cubic box of 64,198 extended a simple point charge (SPC) water molecules [30], and the system was then neutralized by adding thirteen sodium ions. Energy minimization was performed using the steepest descent method of 4000 steps. In the first stage of equilibration, the solute (protein and counter ion) was fixed and position-restrained for 150 ps to relax the protein. Finally, the full system

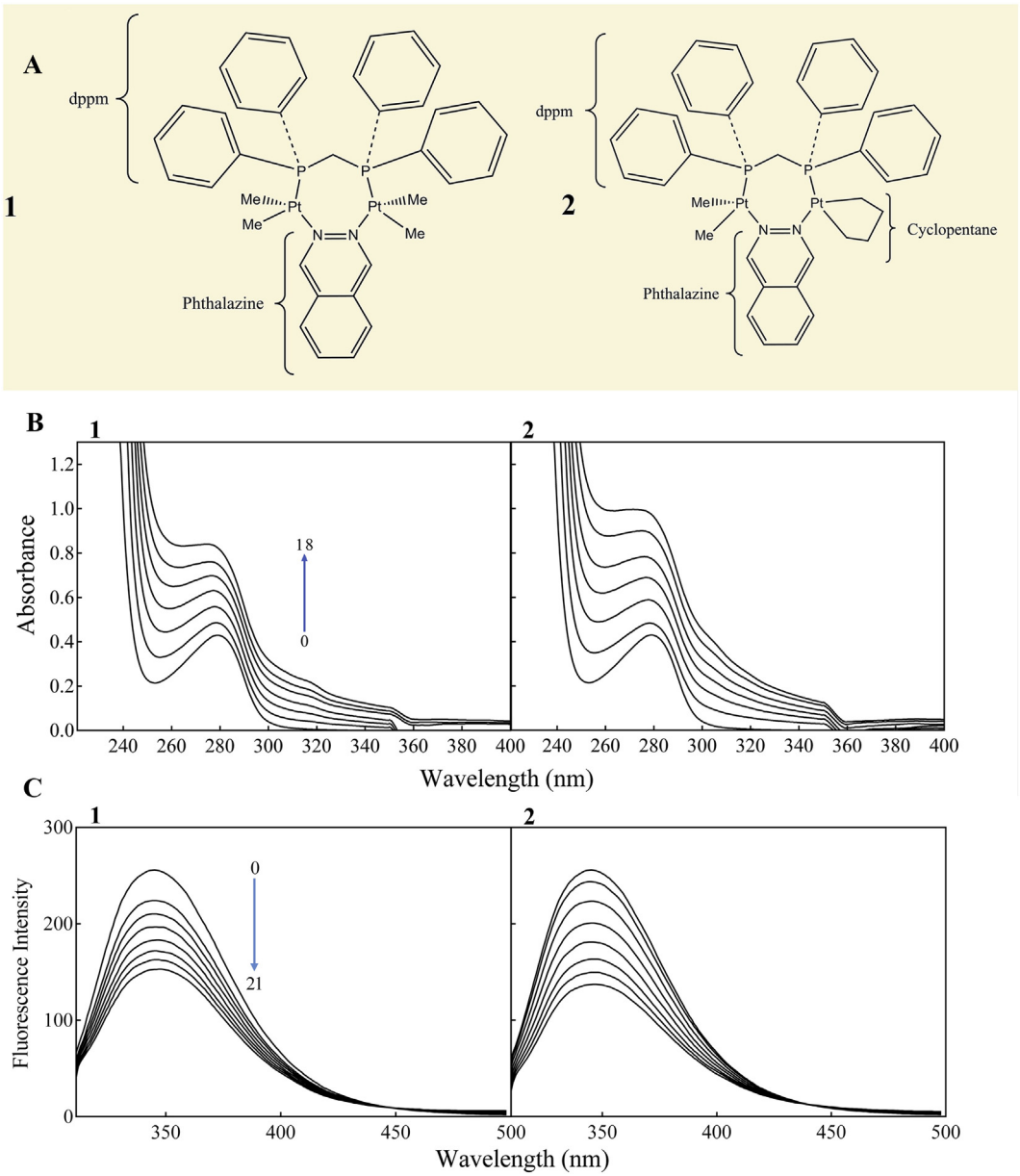

Fig. 2. Chemical structure and spectroscopic characterization of the synthetic complexes. A) Chemical structure of the binuclear Pt (II) complexes. B) UV–Vis absorption spectra of HSA with the increasing concentrations of these complexes. [HSA] = 3 μM, [binuclear Pt (II) complex]: 0–18 μM. The experiments were performed in TN buffer. C) Trp fluorescence analysis of the interaction between binuclear Pt (II) complexes and HSA. The Trp fluorescence emissions of HSA (3 μM) were recorded in the presence of complex **1** and complex **2**, at different concentrations (0–21 μM). The experiments were done in TN buffer at 298 K. The HSA solution was excited at 295 nm and the emission spectra were recorded between 300 and 500 nm. Also, the band slits for excitation and emission were set at 5 and 10 nm, respectively.

was subjected to 20 ns molecular dynamic simulations at 310 K temperature and 1 bar pressure. Also, the periodic boundary condition and integration of motion equations were integrated by applying the leaf-frog algorithm with a time step of 2 fs. The atomic coordinates were recorded at every 1 ps during the simulation for later analysis. The MD simulation and results analysis were performed on Linux Mint 17.6 operating system at the Protein Chemistry Laboratory (PCL).

2.2.11. Molecular Docking Study

Molecular docking was carried out using software Molegro Virtual Docker (MVD) [24]. The structure of each binuclear Pt (II) complex was generated by HyperChem Professional 7.0. Then, energy minimization calculations were carried out with Density Functional Theory (DFT) method in B3LYP level and basis set for Pt and all other atoms adjust to LanL2DZ and 6-31G respectively, using Gaussian 09. The energy minimized Pt (II) complexes and the simulated HSA were imported to the MVD workspace then molecular docking was performed [3].

2.2.12. Statistical Analysis

The experiments were repeated at least three times for each sample, and the statistical differences were determined by a two- tailed student's *t*-test.

3. Results & Discussion

3.1. The UV–Vis Absorption Analysis

As reported previously, the binding profile of drugs to proteins, mostly to serum albumin which functions as a general carrier of the blood stream, is of high importance [13]. In the current study, UV–Vis absorption spectroscopy was used to determine the structural changes

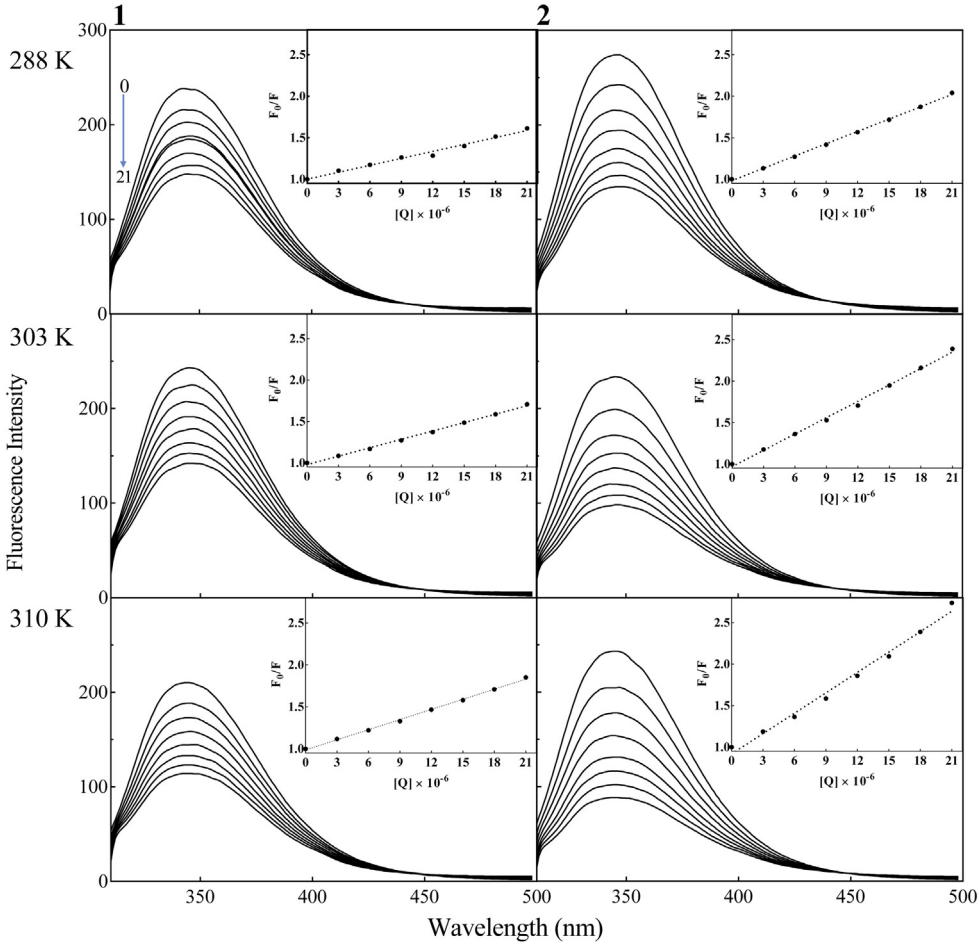

Fig. 3. The temperature dependent fluorescence assessment of interaction between binuclear Pt (II) complexes and HSA. The fluorescence titration experiments were performed with HSA (3.0 μM) and different concentrations of the binuclear Pt (II) complexes (0–21 μM), at different temperatures (288 K, 303 K and 310 K). Inset figure displays the plot of Stern–Volmer fluorescence quenching of HSA by the binuclear Pt (II) complexes at different temperatures. All the experiments were performed in TN buffer, as the wavelength of excitation was fixed at 295 nm, and the emission spectra recorded in the wavelength range of 300 to 500 nm.

of protein and to discover protein-ligand complex formation. Proteins show a broad peak in the region of 250–300 nm of UV–Vis absorption spectrum, consisting of several overlapping bands from the aromatic residues (Trp, Tyr, and Phe), primarily due to π → π* transitions [25]. The UV–Vis absorption studies were carried out in the presence of different concentrations of each binuclear Pt (II) complex (Fig. 2B).

As shown in Fig. 2B, HSA has a strong absorption peak at 280 nm, which increases with the addition of each binuclear Pt (II) complex. Our results suggest that the interaction occurs between HSA and these complexes. Moreover, a blue shift in maximum wavelength of HSA (280 → 277 nm) was observed upon addition of the binuclear Pt (II) complexes. This finding suggests an increase in the polarity of the solvent as a result of the addition of binuclear Pt (II) complexes [26].

Table 1
The quenching constant of Stern–Volmer (K_{sv}) and the rate constant (K_q) for binding of two binuclear Pt (II) complexes to HSA at different temperatures.

Pt (II) complex	T (K)	$K_{sv} \times 10^4$ (M^{-1})	$K_q \times 10^{12}$ ($M^{-1}\,s^{-1}$)	R^a	±SD[b]
1	288	2.45	2.45	0.9855	0.0288
	303	3.19	3.19	0.9970	0.0013
	310	4.20	4.20	0.9980	0.0012
2	288	4.78	4.78	0.9989	0.0010
	303	6.16	6.16	0.9960	0.0065
	310	7.32	7.32	0.9888	0.0198

[a] R is the correlation coefficient.
[b] SD is the standard deviation of three independent measurements.

3.2. Fluorescence Measurements

3.2.1. Intrinsic Fluorescence Measurements

Fluorescence spectroscopy is an important technique to obtain practical information on the protein–ligand interaction [27]. HSA has different fluorophores (Trp, Tyr and Phe residues) and among them, Trp fluorescence reveals the highest sensitivity to the changes in the microenvironment [13]. In this study, the fluorescence spectra of HSA in the absence and presence of different concentrations of each binuclear Pt (II) complex were recorded in the range of 300–500 nm, upon excitation at 295 nm. These complexes cause a concentration-dependent quenching of the intrinsic fluorescence of HSA (Fig. 2C). These results suggest the important interaction between these complexes and albumin. This finding was also confirmed by data of UV–Vis absorption analysis (Fig. 2B).

3.2.2. Fluorescence Quenching Mechanism

The quenching mechanisms occur by two different ways (dynamics and statics) which can be distinguished from each other by their unique temperature-dependent behavior [28,29]. In dynamic quenching, increasing the temperature results in faster diffusion and hence larger amounts of the collision, which subsequently increase the quenching constant. In static quenching, temperature elevation declines the stability of the formed complex and hence reduces the quenching constant [13]. Fluorescence quenching of HSA upon interaction with binuclear Pt (II) complexes was investigated at different temperatures (288,

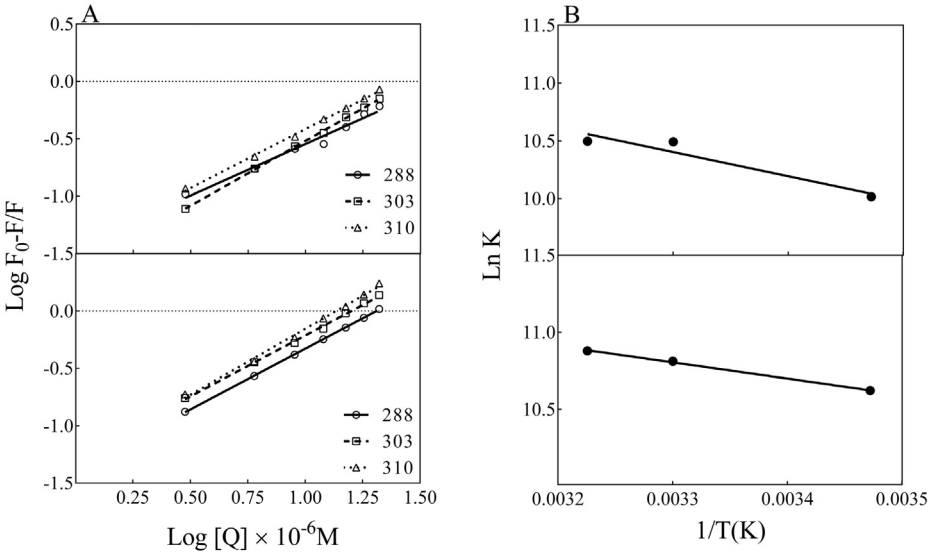

Fig. 4. The plot of log (F_0 / F − 1) against log [Q] and Ln K against 1 / T at three different temperatures. Van't Hoff plot obtained from the interaction between HSA and binuclear Pt (II) complexes is shown. The experiments were done in TN buffer.

303, and 310 K). Fig. 3 shows the plot of fluorescence intensity and F_0 / F (inset figures) versus concentration of each binuclear Pt (II) complex.

As shown in this figure, the Stern–Volmer plots are linear and the slopes increased with rising temperature; consequently value of K_{sv} increased with the temperature elevation in the presence of binuclear Pt(II) complexes, suggesting possible dynamic quenching of HSA fluorescence by the synthetic complexes [3]. By using Eq. (1) the Stern–Volmer constants of the interaction between HSA and these complexes were calculated and the obtained data are summarized in Table 1.

3.2.3. Determination of Association Constant (K_b) and Number of Binding Sites (n)

The values of the association constant (K_b), and the number of binding sites (n), at different temperatures were obtained from the modified Stern–Volmer plots (Fig. 4A). The data were determined using the modified Stern–Volmer equation (Eq. (2)) and the results are presented in Table 2. Since the binding constants (K_b) are increased with rising temperature, the binding occurs in an endothermic fashion [13].

As shown in Table 2, complexes **1** and **2** indicate low and high affinity for HSA, respectively. These findings are in good agreement with the quenching properties of the synthetic complexes. As reported previously, various pharmaceutical parameters of medicines such as distribution, absorption, metabolism, elimination, potency and stability can be enhanced as a result of their interaction with HSA [30]. Therefore, pharmacodynamic and pharmacokinetic properties of drugs are improved with their better binding to this protein. The binding affinity of most drugs lies in the range of 10^4–10^6 M^{-1} [30,31]. The obtained binding affinities for the binuclear Pt (II) complexes are also in the 10^4 M^{-1} order. It means that binding to HSA may affect their pharmacokinetic properties with the same extents as previously reported for some other drugs [32].

Table 2
The association constant (K_b), and number of binding sites (n) for binding of the binuclear Pt (II) complexes to HSA at different temperatures.

Pt (II) complexes	T (K)	$K_b \times 10^4$ (M^{-1})	n	R^a	±SD[b]
1	288	2.24	0.89	0.9792	0.0426
	303	3.60	1.13	0.9991	0.0111
	310	3.62	1.26	0.9979	0.0153
2	288	4.1	1.05	0.9999	0.0037
	303	4.96	1.06	0.9979	0.0156
	310	5.30	1.14	0.9957	0.0246

[a] R is the correlation coefficient.
[b] SD is the standard deviation of three independent measurements.

3.2.4. Forces Involved in the Binding Process

Since the dependence of binding constant on temperature, the thermodynamic process was measured to be accountable for the complex formation between albumin and the synthetic compounds. The physical binding of the macromolecule and small ligands mainly occurs through hydrogen bonding, van der Waals forces, electrostatic- and hydrophobic interactions [13]. In the current study, the thermodynamic parameters of binding were obtained from Van't Hoff plot (Fig. 4B). The equation (Eq. (3)) was used to determine the changes in both enthalpy (ΔH) and entropy (ΔS). Moreover, according to Eq. (4), the changes in binding free energy (ΔG) were calculated as a function of temperature and data are listed in Table 3.

Thermodynamic parameters such as enthalpy (ΔH) and entropy (ΔS) provide significant information on the type of involved interaction forces [13]. The positive values of ΔH and ΔS indicate the role of hydrophobic forces in protein–ligand interaction. Negative Gibbs free energy changes specified the spontaneous nature of the interaction. For a typical hydrophobic interaction, ΔH and ΔS have both positive values. If both parameters are negative, van der Waals and hydrogen interactions have a dominant effect [3]. Moreover, when the binding enthalpies of the binuclear Pt (II) complexes to HSA are positive, the binding process has an endothermic character which can be indicated by the augmentation of K_b values as a function of temperature elevation. As shown in Table 2, the negative value of Gibbs free energy change (ΔG°) means that the interaction process was spontaneous. Additionally, the positive enthalpy (ΔH°) and entropy (ΔS°) values of the interaction of binuclear Pt (II) complexes and HSA indicated that the binding was mainly entropy-driven and the hydrophobic forces play a major role in the reaction [33].

Table 3
Thermodynamic parameters for binding of the binuclear Pt (II) complexes to HSA.

Pt (II) complexes	T (K)	ΔH°/kJ mol^{-1}	ΔS°/J (K mol^{-1})	ΔG°/kJ mol^{-1}
1	288			−23.982
	303	17.37	143.83	−26.428
	310			−27.051
2	288			−25.431
	303	8.76	188.72	−27.234
	310			−28.036

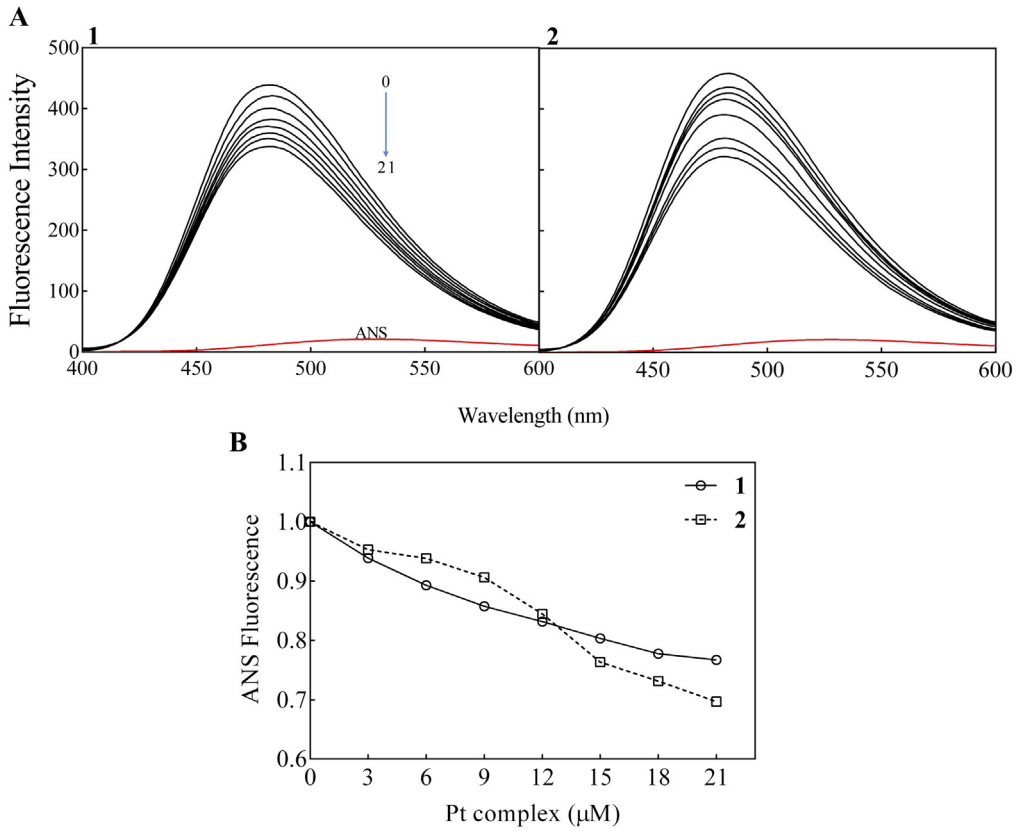

Fig. 5. ANS fluorescence study of the interaction between binuclear Pt (II) complexes and HSA. A) ANS fluorescence intensity of HSA in the presence of increasing concentrations of two binuclear Pt (II) complexes. B) The maximum emission intensity of ANS versus concentration of the synthetic complexes. The experiments were done in the presence of 3 μM HSA and 200 μM ANS. Also, HSA/ANS mixed solutions were excited at 365 nm and the emission spectra were recorded between 400 and 600 nm.

3.2.5. ANS Fluorescence Analysis

ANS, as an extrinsic fluorescent probe, is exceptionally sensitive to the polarity of the solvent. In aqueous solutions, it fluoresces very weak, but upon binding to hydrophobic patches of proteins, its quantum yield increases significantly [28]. Therefore, in this study ANS fluorescence analysis was used for observing possible changes in the protein surface hydrophobicity induced upon interaction with binuclear Pt (II) complexes. For this purpose, a fixed concentration of HSA and ANS was incubated for 20 min in the dark condition before adding various concentrations of each binuclear Pt (II) complex. Fig. 5A indicates that binuclear Pt (II) complexes contest with bound ANS molecules for binding to hydrophobic regions of HSA and causes the detachment of ANS molecules from the hydrophobic surface of HSA, consequently the fluorescence intensity decreases.

As indicated in Fig. 5B, these synthetic complexes compete with almost a similar strength to replace the bound ANS molecules from the protein surface. In addition, the results further approve the contribution of hydrophobic interactions between the synthetic complexes and serum albumin.

3.2.6. Synchronous Fluorescence Measurements

The synchronous fluorescence spectra can offer useful information about the molecular microenvironment in the vicinity of the chromophore in proteins. The synchronous fluorescence analysis of HSA can provide the characteristic information on Tyr and Trp residues when the scanning intervals, Δλ values, between the excitation and emission wavelengths, are fixed at 15 and 60 nm, respectively [29]. The synchronous fluorescence spectra of interaction between binuclear Pt (II) complexes and HSA are presented in Fig. 6.

As shown, the fluorescence intensity of Trp residue is considerably stronger than that of Tyr residues which is an important indication for the major contribution of this amino acid residue in shaping fluorescence intensity profile of human albumin [13]. It was revealed that the fluorescence intensity of HSA decreased regularly along with the addition of each binuclear Pt (II) complex, indicating the occurrence of fluorescence quenching in the binding process. The changes in the maximum emission peak of Tyr or Trp can be judged as conformational changes of the region around these amino acid residues [13,29]. When Δλ set at 15 nm, there was a noticeable red shift of the maximum emission wavelength from 285 to 291 nm in the presence of complex **1**, showing an increase in the polar microenvironment of this residue which may occur as a result of protein unfolding. Also, when Δλ set at 60 nm, there was an apparent red shift of the maximum emission wavelength from 280 to 283 nm, and from 280 nm to 284 nm in the presence of complex **1** and complex **2**, respectively. These observations suggest an important increase in the polarity of the microenvironment of Trp residue. Moreover, there is no significant shift in the maximum emission wavelength of Δλ = 15 nm in the presence of complex **2**, suggesting, interaction of this complex with HSA does not affect the microenvironment of the Tyr residues. The appearance of isosbestic points at Δλ = 15 nm suggests that an equilibrium is established between two species, reflecting the formation of 1:1 complexes between free fluorophores (binuclear Pt (II) complexes) and Tyr [34].

3.2.7. The Competitive Displacement Analyses

In order to elucidate the binding site of these complexes on HSA, competitive binding displacement analysis was performed. Warfarin and ibuprofen are two markers specific for sites I (subdomains IIA) and II (subdomains IIIA), respectively (see Fig. 1). Therefore, to determine the location of each binuclear Pt (II) complex on HSA, the competitive displacement experiment was carried out using warfarin as a characteristic marker for the site I (Fig. 7A) and ibuprofen specific for site II (Fig. 7B). The fluorescence spectra of ternary mixtures of each

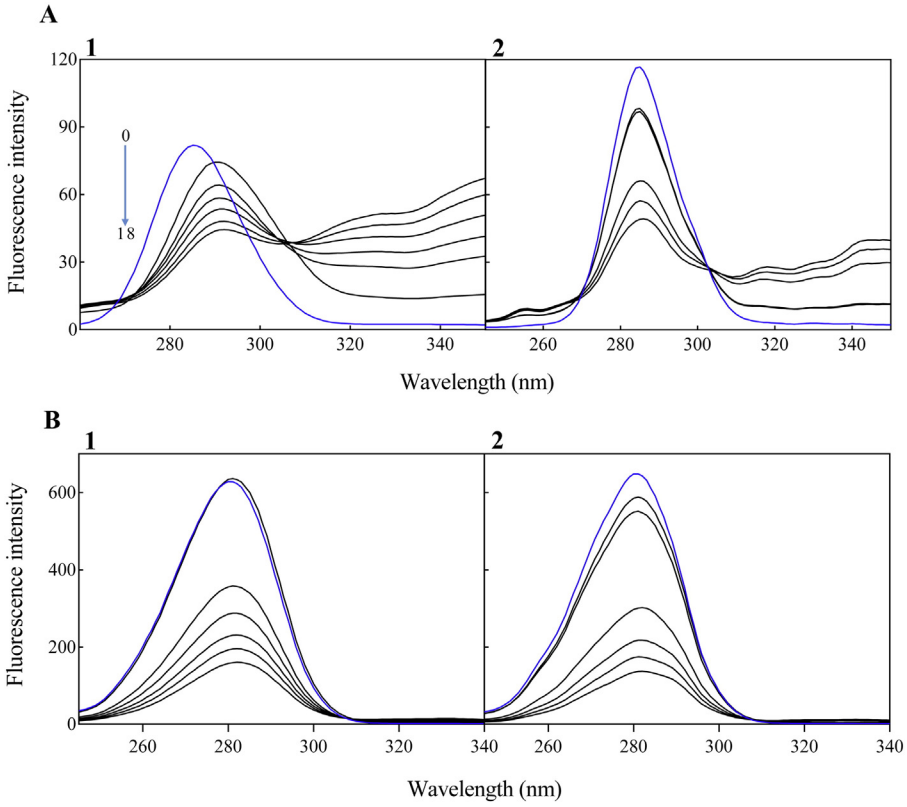

Fig. 6. Synchronous fluorescence analysis of the interaction between HSA and the synthetic binuclear Pt (II) complexes. A) Synchronous fluorescence spectra are shown at $\Delta\lambda = 15$ nm. B) Synchronous fluorescence spectra are shown at $\Delta\lambda = 60$ nm. Synchronous fluorescence profiles of HSA were obtained in the absence and presence of various concentrations of each binuclear Pt (II) complex. The experiments performed in the presence of a fixed concentration of HSA (3.0 μM) and increasing concentrations of each binuclear Pt (II) complex (0–18 μM) in TN buffer. The details of this experiment are discussed in the experimental section.

binuclear Pt (II) complex, HSA and site markers were shown in Fig. 7 at 298 K with the excitation wavelength at 295 nm.

In this experiment, binuclear Pt (II) complexes were gradually added to the solution of HSA–ibuprofen or HSA–warfarin, and then the fluorescence spectra were collected. The results indicated that the fluorescence intensity of the HSA–marker systems was decreased to different degrees. To compare more precisely the effect of complexes on each site marker–HSA system, the fluorescence data were analyzed by a

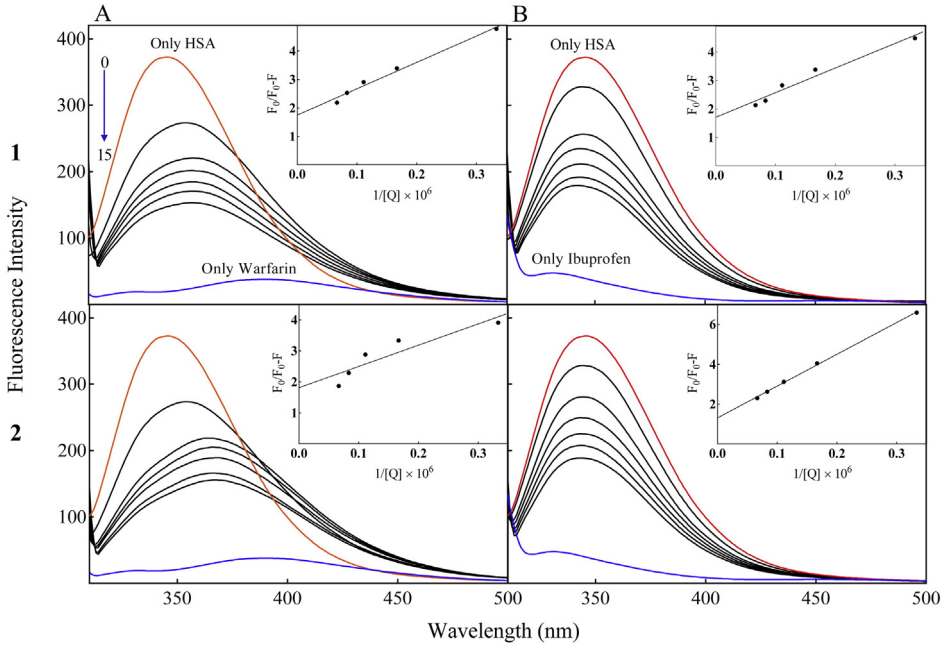

Fig. 7. The competitive displacement of warfarin and ibuprofen with the synthetic binuclear Pt (II) complexes. The ability of binuclear Pt (II) complexes was measured on the fluorescence quenching of HSA-warfarin complex (A) and HSA-ibuprofen complex (B) in TN buffer. [HSA] = [warfarin or ibuprofen] = 3 μM, [Pt complex] = 0–15 μM. All reproduced data were representative of at least three independent determinations. Inset figure shows fluorescence quenching data of HSA, HSA-ibuprofen, and HSA-warfarin in the presence of various concentration of each binuclear Pt (II) complex.

Table 4
The association constants for binding of the binuclear Pt (II) complexes to HSA.

	K_a ($\times 10^5$ L mol^{-1})	
	1	**2**
HSA + W	1.89 ± 0.1217	1.98 ± 0.3207
HSA + I	2.64 ± 0.3360	0.82 ± 0.0581
R(W/I)	0.9843/0.9639	0.8318/0.9988

R: correlation coefficient, W: warfarin, I: Ibuprofen.

modified Stern–Volmer (Eq. (5)), and the corresponding association constants were indicated in Table 4. According to results, the association constant of warfarin–HSA system decreased remarkably in the presence of binuclear Pt (II) complex **2**, while it had a negligible reduction with the addition to the ibuprofen–HSA system. As shown in Scheme 1 our results suggested that warfarin was displaced from its binding site by complex **2**. Therefore, we propose that this binuclear Pt (II) complex interacts with site I on HSA. In a similar way, complex **1** mostly displaces ibuprofen from site II on this protein (Scheme 1).

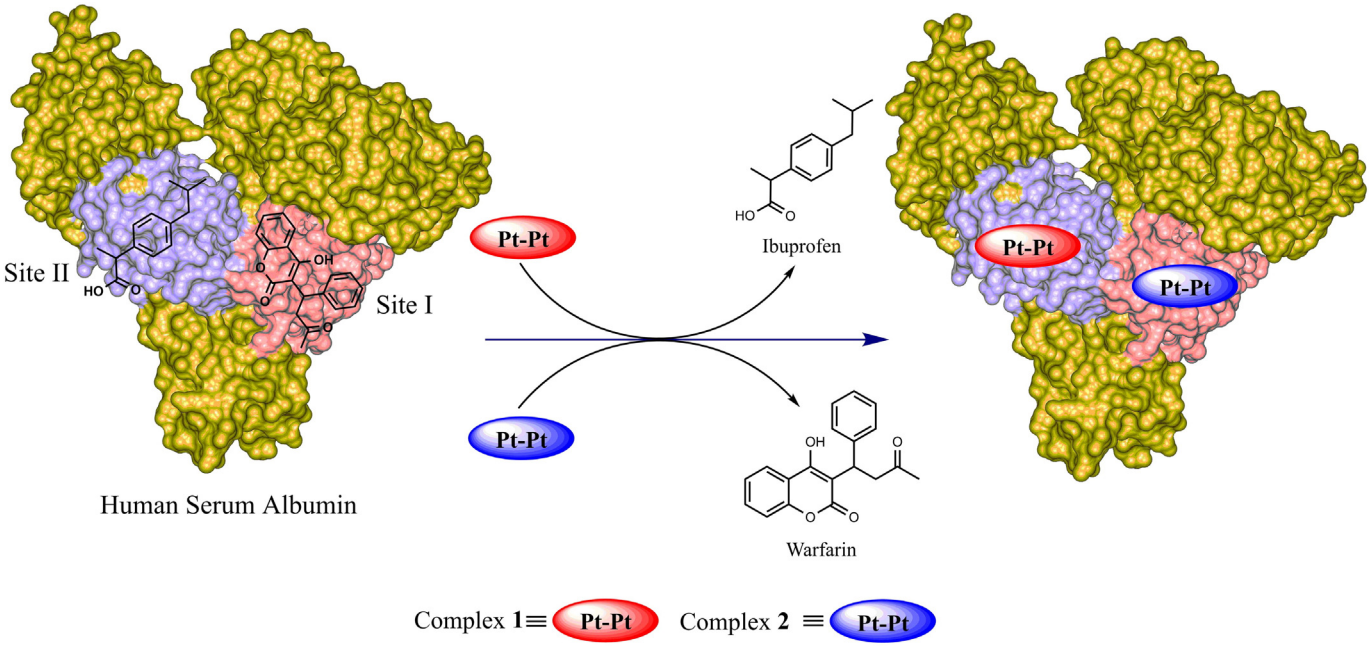

Scheme 1. Displacement of the synthetic binuclear Pt (II) complexes on HSA by ibuprofen and warfarin. The binuclear Pt (II) complexes **1** and **2** preferentially displace ibuprofen and warfarin from the drug binding sites II and I on human albumin, respectively.

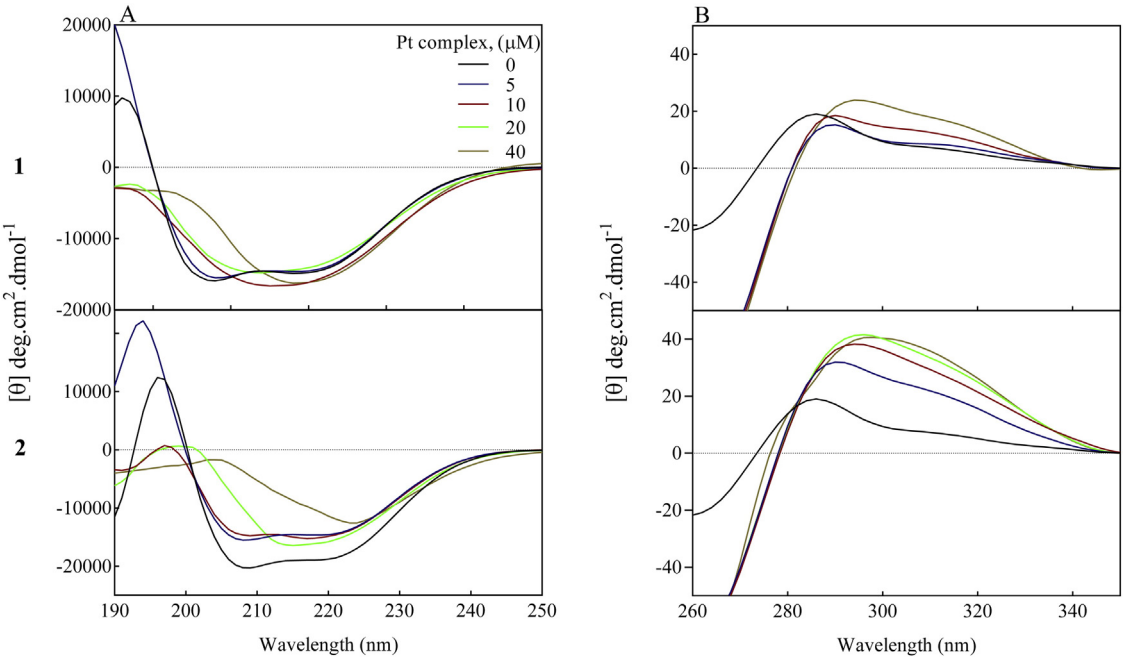

Fig. 8. Far- and near-UV CD analysis of HSA in the presence of various concentrations of each binuclear Pt (II) complex. The experiments were done in the presence of a fixed HSA concentration (1 mg/mL) and different concentrations of each binuclear Pt (II) complex (0–40 μM). The details of this experiment are discussed in the experimental section.

Table 5
The changes in secondary structure of HSA upon interaction with the binuclear Pt (II) complexes.

Pt (II) complex	(μM)	α-helix (%)	β-sheet (%)	β-turn (%)	Random coil (%)
1	0	61.7	7.6	12.9	17.8
	5	58.7	8.9	13.8	18.6
	10	52.8	10.2	14.3	22.7
	20	49.0	12.5	14.9	23.6
	40	26.2	24.0	17.3	32.5
2	0	61.7	7.6	12.9	17.8
	5	49.9	10.6	15.3	24.2
	10	47.8	11.3	16.2	24.7
	20	29.0	21.3	17.4	32.3
	40	17.2	24.2	18.4	40.2

The mean value of three individual experiments with standard ranges from 0.03 to 0.09.

3.3. Circular Dichroism Analysis

The CD spectroscopy is a delicate technique to screen the conformational changes in the protein. Far- and near-UV CD spectra can be used to elucidate the secondary structure and side-chain environments of proteins, respectively [3]. The negative bands at 208 and 222 nm of CD spectra are representative of the right-handed α-helical structures. The rational description is that the negative peaks between 208 and 209 nm and between 222 and 223 nm are both contributed to n → π* transfer for the peptide bonds of α-helical structures of HSA [21]. The far-UV CD spectrum of HSA (Fig. 8A) shows a domination of typical α-helix structure with a broad negative minimum around 209 nm. Because of interaction between HSA and binuclear Pt (II) complexes, the far-UV CD spectra display roughly variation to that of native HSA, suggesting that binding of these complexes to HSA had a significant effect on the protein secondary structures.

The near-UV CD spectra of native HSA showed a regularly increase of the absorption peak in the range of 280–330 nm, with increasing concentration of the binuclear Pt (II) complexes, suggesting that the interaction of these complexes with HSA disrupts the anisotropic environment of Trp residues (Fig. 8B) [3]. The results of deconvolution of CD spectra as presented in Table 5, display that upon interaction with these complexes, the loss of α-helical content is reorganized in the secondary structures with a slight favorite for antiparallel β-sheet and random coil structures. The loss of the α-helix, in favor of the β-sheet and turn structures suggests unfolding of HSA that occurs in the presence of these synthetic complexes [35]. As shown in Fig. 8, conformational changes in HSA which induced by complex **2** is more significant than complex **1**, reflecting with the larger binding constant of complex **2** in comparison to complex **1**. The CD results are also in good agreement with the results of fluorescence and UV–Vis assessments.

3.4. Molecular Docking Simulation Study

In order to acquire the simulated crystal structure of HSA (4L8U) in unliganded form, the protein was subjected to 20 ns MDS, in neutralized water box at 310 K and 1 bar pressure. The root mean square deviation

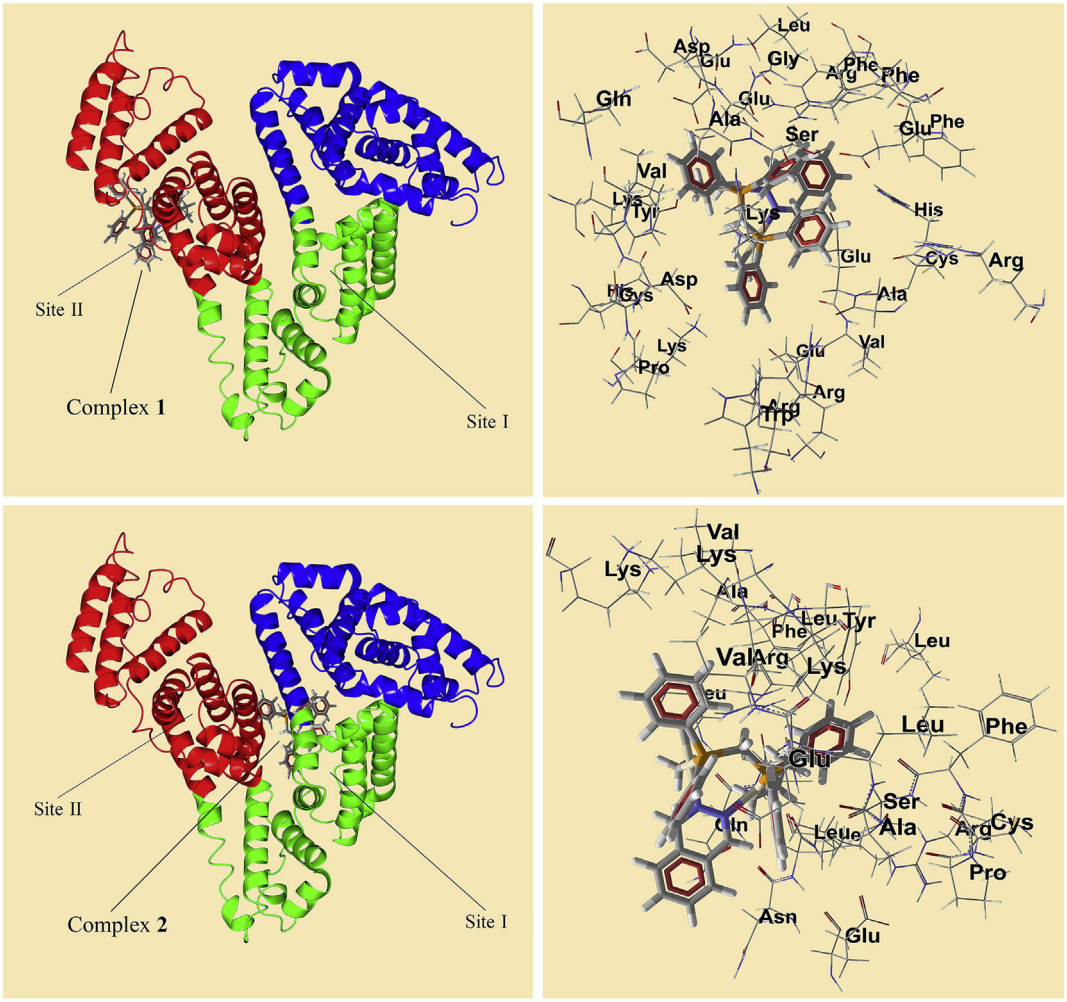

Fig. 9. The protein binding sites and amino acid residues involved in the interaction with the synthetic binuclear Pt (II) complexes.

Table 6
The energy of interaction between binuclear Pt (II) complexes and responsive amino acid residues in molecular docking analysis.

Complex **1**		Complex **2**	
Amino acid residues	Interaction energies (kJ mol^{-1})	Amino acid residues	Interaction energies (kJ mol^{-1})
Ala-191	−2.39289	Ala-490	−8.58227
Ala-291	−3.68916	Arg-410	−25.299
Arg-160	−2.0279	Asn-391	−6.00255
Arg-218	−11.80535	Gln-390	−12.3769
Arg-222	−10.85325	Glu-492	−4.80568
Asp-187	−1.55004	Leu-387	−0.78717
Asp-451	−4.4078	Leu-491	−8.71636
Glu-153	−3.34791	Lys-413	−1.07038
Glu-184	−2.63248	Lys-414	−1.91378
Glu-188	−3.6525	Phe-488	−10.30923
Glu-292	−7.56334	Ser-489	−3.84194
His-288	−5.58214	Tyr-411	−4.54848
Lys-195	−3.43386	Val-493	−1.99164
Lys-436	−1.64169		
Phe-157	−4.8548		
Ser-192	−3.71535		
Tyr-452	−3.71602		
Val-455	−2.41602		
Total interaction energy: −79.28		Total interaction energy: −90.24	

(RMSD) values of atoms in HSA with respect to the initial one was plotted versus time to elucidate the time that system reaches its equilibrium state. HSA has endured a fluctuating value of RMSD around the constant average of 0.11 nm from 15 to 20 ns (Fig. S).

Therefore, the final structure was proposed to the docking simulation study. Molecular docking simulation was performed with the aim to clarify the binding sites of the binuclear Pt (II) complexes on HSA, binding affinity and defining the driving forces. The docking results as presented in Fig. 9, the best binding mode of complex **1** is placed in domain III in the cleft between subdomains IIIA and IIIB of the protein (mostly in IIIA; drug site II).

On the other hand, complex **2** prefers lying in the area between subdomains IA, IIA and IIA of the protein (mostly in IIA; drug site I). This result is in good agreement with the results of competitive displacement assay (see Fig. 7). Additionally, the interaction energies between different amino residues of HSA and synthetic binuclear Pt (II) complexes are listed in Table 6. The data indicated that Arg-218, Arg-222, Glu-292 and His-288 in subdomain IIA, as well as Val-493, Phe-488, Leu-491, Ala-490 and Asn-391 in subdomain IIIA interact effectively with the binuclear Pt (II) complexes **1** and **2**, respectively. A π–π stacking exists between aromatic rings of the complexes and Phe-157, Phe-488 and Tyr-411, Tyr-452 in HSA. Hydrophobic interactions between these complexes and Ala-191, Ala-291, Ala-490, Val-455, Val-493 and Leu-491 are indicated in their binding to HSA. It means that no electrostatic or hydrogen bonding can be predicted as supported by positive enthalpy and entropy values achieved in our experimental results.

4. Conclusion

The interactions between two binuclear Pt (II) complexes and HSA were studied by the aid of different biophysical techniques and molecular docking analysis. Moreover, the assessments revealed that binding of these complexes to HSA occurred mainly via entropy driven hydrophobic force, which accompanied with the protein partial unfolding at a relatively high concentration of these complexes. On the other hand, complex **1** demonstrated the worthy affinity and least denaturing effect on HSA. Due to its low denaturing effect on the protein and considering its significant anticancer activity, as indicated in our previous study, this complex could represent potentially a reasonable molecular template for the future designing of anticancer binuclear Pt (II) complexes.

Supplementary data to this article can be found online at http://dx.doi.org/10.1016/j.jphotobiol.2016.09.035.

Conflict of interest

The authors declare that they have no conflicts of interest with the contents of this article.

Acknowledgments

RY and SA appreciatively acknowledge the financial supports of their Universities Research Councils. In addition, we would like to appreciate the financial supports of Iran National Science Foundations (Grant nos. 94016326 and 92001695).

References

[1] A.-M. Florea, D. Büsselberg, Cisplatin as an anti-tumor drug: cellular mechanisms of activity, drug resistance and induced side effects, Cancers 3 (2011) 1351–1371.
[2] A.M. Pizarro, P.J. Sadler, Unusual DNA binding modes for metal anticancer complexes, Biochimie 91 (2009) 1198–1211.
[3] R. Yousefi, R. Mohammadi, A. Taheri-Kafrani, M.B. Shahsavani, M. Dadkhah Aseman, S.M. Nabavizadeh, M. Rashidi, N. Poursasan, A.A. Moosavi-Movahedi, Study of the interaction between two newly synthesized cyclometallated platinum (II) complexes and human serum albumin: spectroscopic characterization and docking simulation, J. Lumin. 159 (2015) 139–146.
[4] Y.J. Hu, Y. Liu, T.Q. Sun, A.M. Bai, J.Q. Lu, Z.B. Pi, Binding of anti-inflammatory drug cromolyn sodium to bovine serum albumin, Int. J. Biol. Macromol. 39 (2006) 280–285.
[5] N. Seedher, S. Bhatia, Reversible binding of celecoxib and valdecoxib with human serum albumin using fluorescence spectroscopic technique, Pharmacol. Res. 54 (2006) 77–84.
[6] X. Li, S. Wang, Study on the interaction of (+)-catechin with human serum albumin using isothermal titration calorimetry and spectroscopic techniques, New J. Chem. 39 (2015) 386–395.
[7] D. Li, J. Zhu, J. Jin, X. Yao, Studies on the binding of nevadensin to human serum albumin by molecular spectroscopy and modeling, J. Mol. Struct. 846 (2007) 34–41.
[8] F. Keshavarz, M.M. Alavianmehr, R. Yousefi, Molecular interaction of benzalkonium ibuprofenate and its discrete ingredients with human serum albumin, Phys. Chem. Res. 1 (2013) 111–116.
[9] T.K. Maiti, K.S. Ghosh, J. Debnath, S. Dasgupta, Binding of all-trans retinoic acid to human serum albumin: fluorescence, FT-IR and circular dichroism studies, Int. J. Biol. Macromol. 38 (2006) 197–202.
[10] Y. Wang, H. Yu, X. Shi, Z. Luo, D. Lin, M. Huang, Structural mechanism of ring-opening reaction of glucose by human serum albumin, J. Biol. Chem. 288 (2013) 15980–15987.
[11] M.X. Xie, M. Long, Y. Liu, C. Qin, Y.D. Wang, Characterization of the interaction between human serum albumin and morin, Biochim. Biophys. Acta 1760 (2006) 1184–1191.
[12] C.D. Kanakis, P.A. Tarantilis, M.G. Polissiou, S. Diamantoglou, H.A. Tajmir-Riahi, Antioxidant flavonoids bind human serum albumin, J. Mol. Struct. 798 (2006) 69–74.
[13] R. Yousefi, M. Jamshidi, M.B. Shahsavani, S.M. Nabavizadeh, M.G. Haghighi, M. Rashidi, A. Taheri-Kafrani, A. Niazi, F. Keshavarz, M.M. Alavinamehr, Study on the interaction of three structurally related cationic Pt(II) complexes with human serum albumin: importance of binding affinity and denaturing properties, J. Iran. Chem. Soc. 1-14 (2015).
[14] Y.Z. Zhang, H.R. Li, J. Dai, W.J. Chen, J. Zhang, Y. Liu, Spectroscopic studies on the binding of cobalt(II) 1,10-phenanthroline complex to bovine serum albumin, Biol. Trace Elem. Res. 135 (2010) 136–152.
[15] A. Sułkowska, Interaction of drugs with bovine and human serum albumin, J. Mol. Struct. 614 (2002) 227–232.
[16] B. Zhou, Z.-D. Qi, Q. Xiao, J.-X. Dong, Y.-Z. Zhang, Y. Liu, Interaction of loratadine with serum albumins studied by fluorescence quenching method, J. Biochem. Biophys. Methods 70 (2007) 743–747.
[17] M.B. Shahsavani, S. Ahmadi, M.D. Aseman, S.M. Nabavizadeh, M. Rashidi, Z. Asadi, N. Erfani, A. Ghasemi, A.A. Saboury, A. Niazi, A. Bahaoddini, R. Yousefi, Anticancer activity assessment of two novel binuclear platinum (II) complexes, J. Photochem. Photobiol. B 161 (2016) 345–354.
[18] S.J. Hoseini, S.M. Nabavizadeh, S. Jamali, M. Rashidi, Uncommon solvent effect in oxidative addition of mei to a new dinuclear platinum complex containing a platina(II) cyclopentane moiety, Eur. J. Inorg. Chem. 2008 (2008) 5099–5105.
[19] S. Jamali, S.M. Nabavizadeh, M. Rashidi, Oxidative addition of methyl iodide to a new type of binuclear platinum(II) complex: a kinetic study, Inorg. Chem. 44 (2005) 8594–8601.
[20] F. Ding, N. Li, B. Han, F. Liu, L. Zhang, Y. Sun, The binding of C.I. Acid Red 2 to human serum albumin: determination of binding mechanism and binding site using fluorescence spectroscopy, Dyes Pigm. 83 (2009) 249–257.
[21] G. Zhang, Y. Ma, Mechanistic and conformational studies on the interaction of food dye amaranth with human serum albumin by multispectroscopic methods, Food Chem. 136 (2013) 442–449.

[22] P. Bourassa, S. Dubeau, G.M. Maharvi, A.H. Fauq, T.J. Thomas, H.A. Tajmir-Riahi, Binding of antitumor tamoxifen and its metabolites 4-hydroxytamoxifen and endoxifen to human serum albumin, Biochimie 93 (2011) 1089–1101.
[23] A. Divsalar, A.A. Saboury, R. Yousefi, A.A. Moosavi-Movahedi, H. Mansoori-Torshizi, Spectroscopic and cytotoxic studies of the novel designed palladium(II) complexes: β-lactoglobulin and K562 as the targets, Int. J. Biol. Macromol. 40 (2007) 381–386.
[24] R. Thomsen, M.H. Christensen, MolDock: a new technique for high-accuracy molecular docking, J. Med. Chem. 49 (2006) 3315–3321.
[25] L.H. Lucas, B.A. Ersoy, L.A. Kueltzo, S.B. Joshi, D.T. Brandau, N. Thyagarajapuram, L.J. Peek, C.R. Middaugh, Probing protein structure and dynamics by second-derivative ultraviolet absorption analysis of cation–π interactions, Protein Sci. 15 (2006) 2228–2243.
[26] F.-X. Schmid, Biological macromolecules: UV-visible spectrophotometry, eLS, John Wiley & Sons, Ltd, 2001.
[27] F. Ding, W. Liu, J.-X. Diao, B. Yin, L. Zhang, Y. Sun, Complexation of insecticide chlorantraniliprole with human serum albumin: biophysical aspects, J. Lumin. 131 (2011) 1327–1335.
[28] M. Möller, A. Denicola, Study of protein-ligand binding by fluorescence, Biochem. Mol. Biol. Educ. 30 (2002) 309–312.
[29] G. Zhang, N. Zhao, L. Wang, Fluorescence spectrometric studies on the binding of puerarin to human serum albumin using warfarin, ibuprofen and digitoxin as site markers with the aid of chemometrics, J. Lumin. 131 (2011) 2716–2724.
[30] I. Petitpas, A.A. Bhattacharya, S. Twine, M. East, S. Curry, Crystal structure analysis of warfarin binding to human serum albumin: anatomy of drug site I, J. Biol. Chem. 276 (2001) 22804–22809.
[31] J. Ghuman, P.A. Zunszain, I. Petitpas, A.A. Bhattacharya, M. Otagiri, S. Curry, Structural basis of the drug-binding specificity of human serum albumin, J. Mol. Biol. 353 (2005) 38–52.
[32] M.J. Yoo, Q.R. Smith, D.S. Hage, Studies of imipramine binding to human serum albumin by high-performance affinity chromatography, J. Chromatogr. B Analyt. Technol. Biomed. Life Sci. 877 (2009) 1149–1154.
[33] S.S. Kalanur, J. Seetharamappa, V.K. Kalalbandi, Characterization of interaction and the effect of carbamazepine on the structure of human serum albumin, J. Pharm. Biomed. Anal. 53 (2010) 660–666.
[34] C. Bhaumik, D. Saha, S. Das, S. Baitalik, Synthesis, structural characterization, photophysical, electrochemical, and anion-sensing studies of luminescent homo- and heteroleptic ruthenium(II) and osmium(II) complexes based on terpyridyl-imidazole ligand, Inorg. Chem. 50 (2011) 12586–12600.
[35] J.T. Pelton, L.R. McLean, Spectroscopic methods for analysis of protein secondary structure, Anal. Biochem. 277 (2000) 167–176.